Supporting information

Micro and Nanocrystalline Inverse Spinel LiCoVO$_4$ for Intercalation Pseudocapacitive Li$^+$ Storage with Ultrahigh Energy Density and Long-Term Cycling

Haritha Hareendrakrishnakumar, Reshma Chulliyote, and Mary Gladis Joseph*

Department of Chemistry, Indian Institute of Space Science and Technology, Valiyamala, Thiruvananthapuram 695 547, India

Corresponding Author*: marygladis@iist.ac.in

Electrochemical Measurements

The mass loading ratio between positive and negative electrodes in the asymmetric supercapacitor (full-cell) was optimized according to the specific capacitance calculated from their discharge curves and can be expressed as follows:

$$\frac{m_+}{m_-} = \frac{C_- \times V_-}{C_+ \times V_+} \qquad (1)$$

where m (g) is the mass of active material in positive and negative electrode, C (F g^{-1}) is the specific capacitance of single electrode calculated using (2), and ΔV (V) is the operating potential of each electrodes.

Specific capacitance can be calculated from the discharge curves according to the following equation:

$$C = \frac{I \times \Delta t}{m \times \Delta V} \qquad (2)$$

where C (F g^{-1}) is the specific capacitance calculated based on the mass of the active material, I (A) is the constant discharge current, Δt (s) is the discharge time, ΔV (V) is the discharge voltage excluding the IR drop, and m (g) is the mass of active material coated on the individual electrode for 3-elctrode setup or the total mass of active materials on the two electrodes for full-cell setup.

Energy density and power density were calculated according to the following equations:

$$E = \frac{1}{2} CV^2 \qquad (3)$$

$$P = \frac{E}{t} \qquad (4)$$

where C (F g^{-1}) is the specific capacitance of the full-cell, V (V) is the operating potential of the cell, t (s) is the discharge time, E (Wh kg^{-1}) is the energy density, and P (kW kg^{-1}) is the power density.

Calculation of average crystallite size from powder XRD using Scherrer equation

The average crystallite size of S-LCVO and H-LCVO were calculated from the full width at half maximum (FWHM) of the diffraction peak using Scherrer equation:

$$D = \frac{K\lambda}{\beta\,Cos\,\theta}$$

where D (nm) is the average crystallite size,

K is the Scherrer constant, 0.94 for cubic crystal structure,

λ is the wavelength of Cu-Kα radiation (0.15406 nm),

β (radian) is the full width at half maximum of the peak corresponding to (311) plane,

θ is the angle obtained from 2θ value corresponding to the maximum intensity peak.
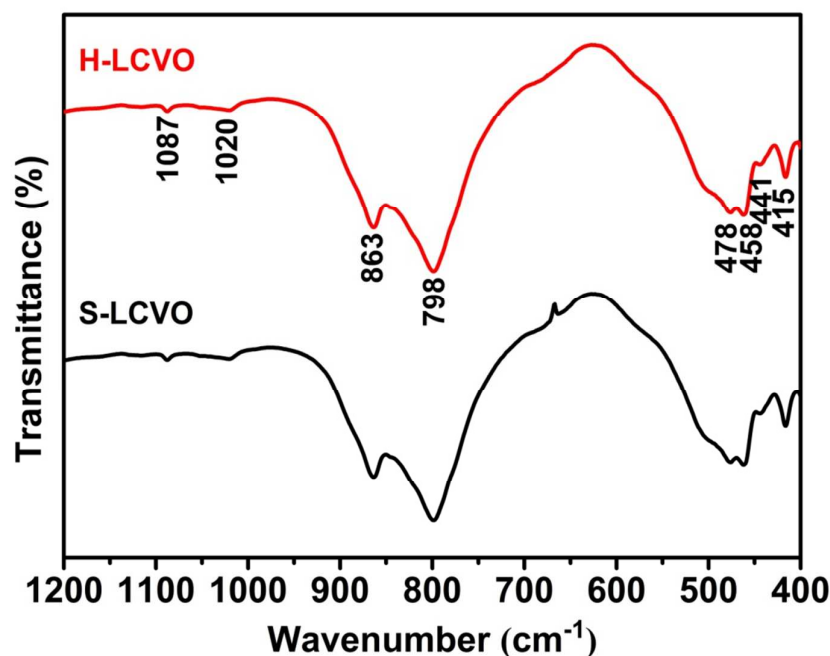
Figure S1. FT-IR spectrum of solid state (S-LCVO) and hydrothermally (H-LCVO) derived LiCoVO$_4$

FT-IR spectrum of LiCoVO$_4$ synthesized via solid-state and hydrothermal reaction in the wave number ranging from 400 to 1200 cm^{-1} is represented in Fig. S1. The absorption band observed at 863 and 798 cm^{-1} are assigned to the stretching vibrations of VO$_4$ tetrahedrons. The bands sited around 600 to 450 cm^{-1} region are associated with the vibrations of Ni-O bonds in NiO$_6$ and Li-O bonds in LiO$_6$ octahedral units or bending vibrations of VO$_4$ tetrahedron. The two weak absorption bands observed at 1087 and 1020 cm^{-1} corresponds to the asymmetric stretching vibration mode of Ni-O bonds in NiO$_6$ octahedron. The two weak bands around 441 and 415 cm^{-1} refer to asymmetric stretching vibrations of Li-O bonds in LiO$_6$ octahedron.[1]

References:

1. Bhuvaneswari, M. S.; Selvasekarapandian, S.; Kamishima, O.; Kawamura, J.; Hattori, T.; Vibrational Analysis of Lithium Nickel Vanadate, *J. Power Sources* **2005**, *139*, 279-283.
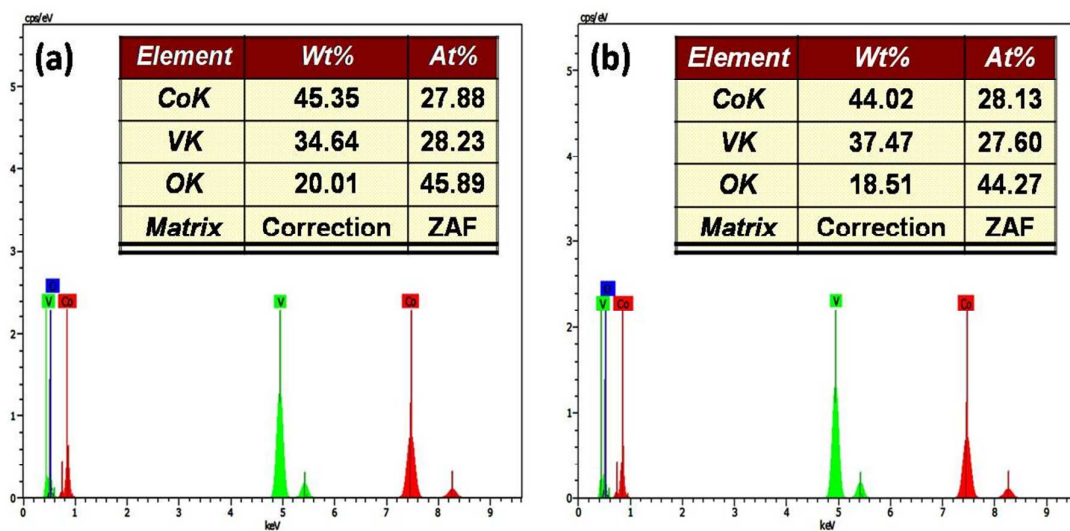
Element	Wt%	At%
CoK	45.35	27.88
VK	34.64	28.23
OK	20.01	45.89
Matrix	Correction	ZAF

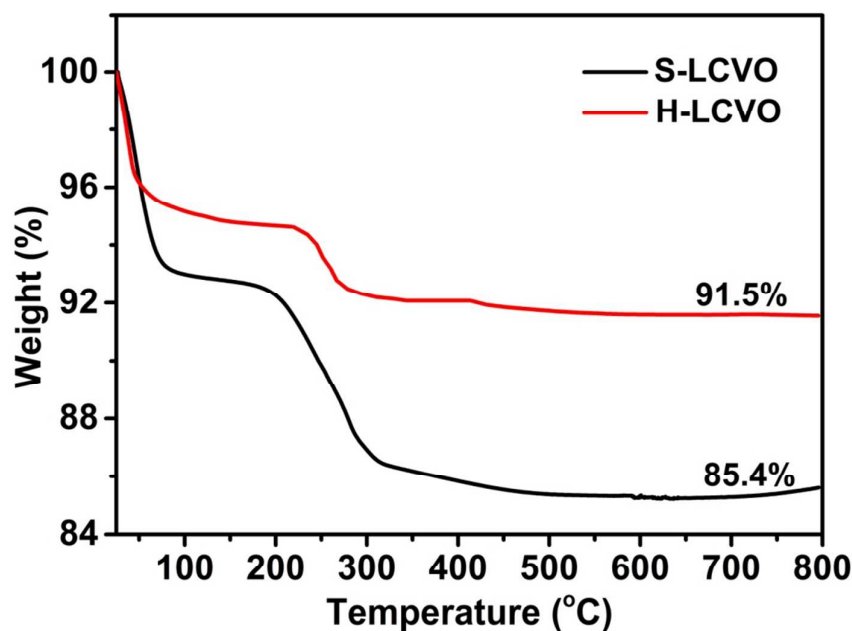| Element	Wt%	At%
CoK	44.02	28.13
VK	37.47	27.60
OK	18.51	44.27
Matrix	Correction	ZAF

Figure S2. EDS spectrum of (a) S-LCVO (b) H-LCVO

Figure S3. TGA curves of S-LCVO and H-LCVO

Fig. S3 shows the thermal decomposition profile of S-LCVO and H-LCVO in a temperature range of 25 to 800 °C. The initial weight loss below 100 °C is attributed to the evaporation of residual water. The next weight loss observed in the temperature range of 200 to 300 °C is due to the decomposition of residual precursor materials, which takes place at its melting points. After 300 °C, both S-LCVO and H-LCVO gives a stable decomposition curve. The percentage weight loss until the weight stabilizes is 14.6% for S-LCVO and 8.5% for H-LCVO.
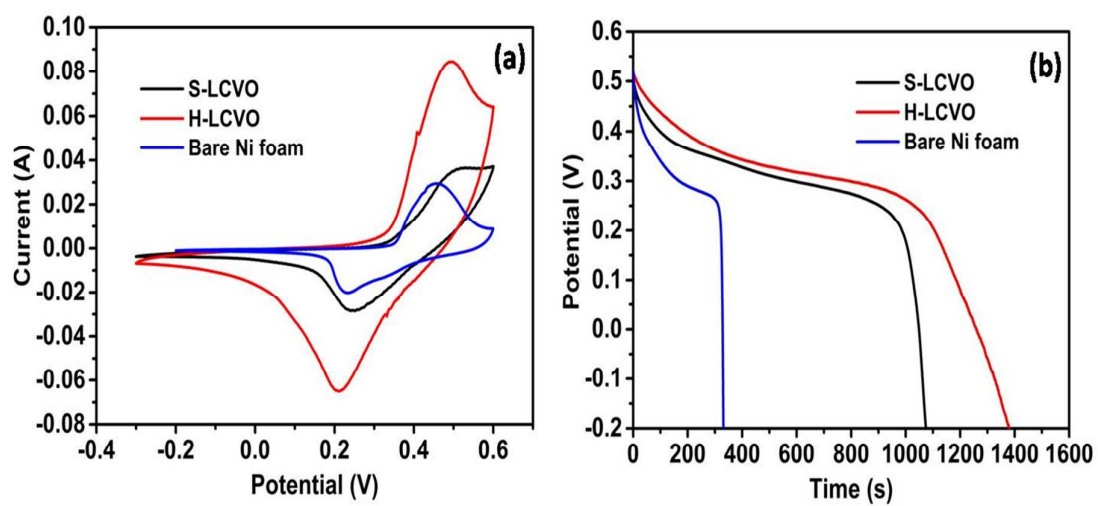
Figure S4. (a) CV curves of S-LCVO, H-LCVO, and bare Ni foam substrate at the same sweep rate of 100 mV s^{-1} (b) Galvanostatic discharge curves of S-LCVO, H-LCVO, and bare Ni foam substrate at the same sweep rate of 0.5 A g^{-1}.
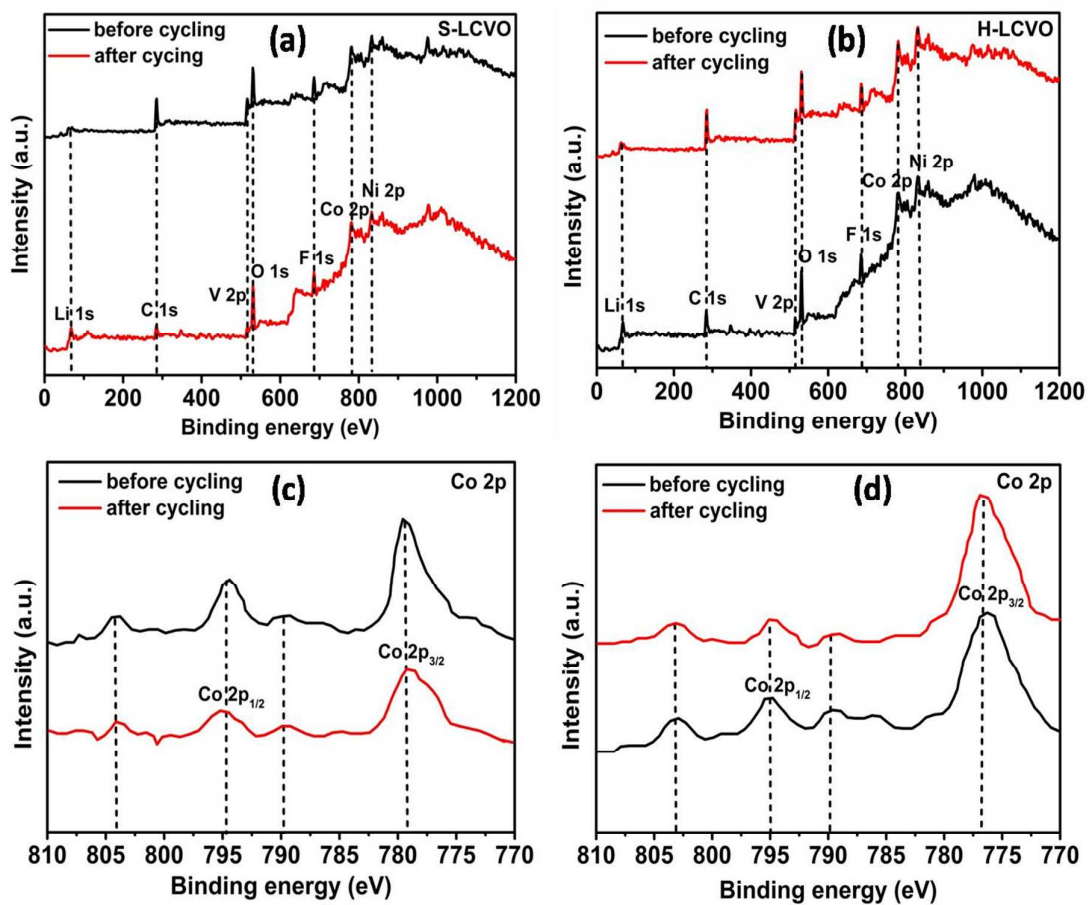
Figure S5. XPS survey spectrum of (a) S-LCVO electrode before and after cycling (b) H-LCVO electrode before and after cycling. Comparative XPS core level spectrum of Co 2p (c) S-LCVO electrode before and after cycling (d) H-LCVO electrode before and after cycling
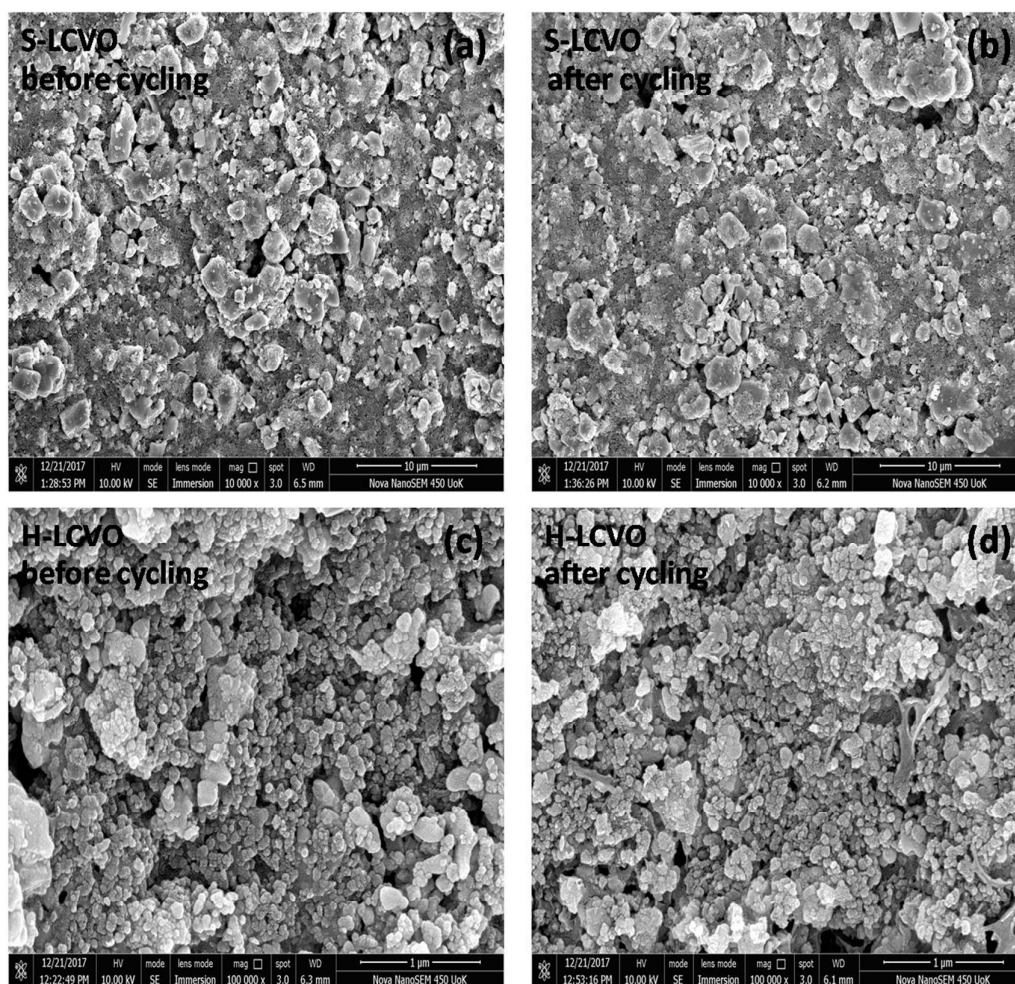
Figure S6. FESEM images: S-LCVO (a) before cycling (b) after cycling and H-LCVO (c) before cycling (d) after cycling
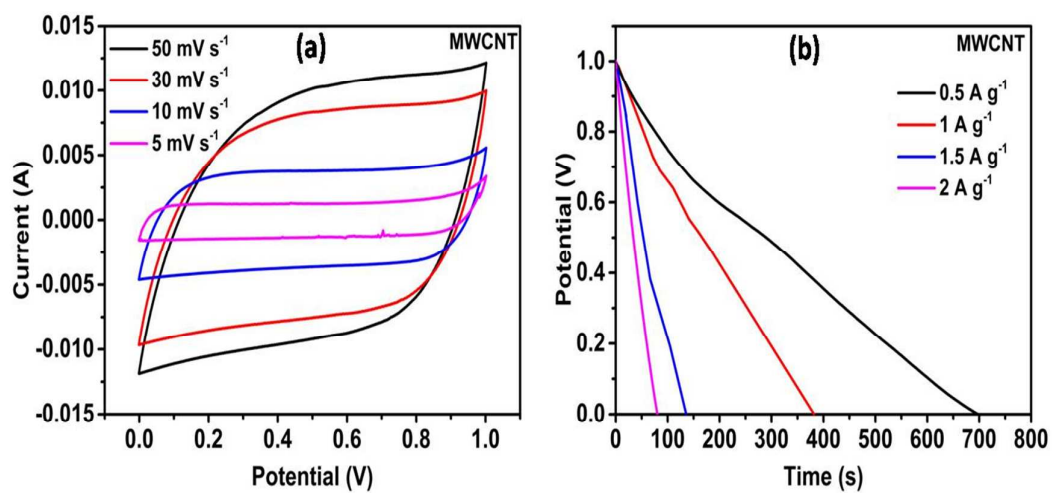
Figure S7. Electrochemical evaluation of MWCNT electrode in 1 M LiOH electrolyte: (a) CV curves at different potential sweep rates (b) galvanostatic discharge curves at different applied current densities.